INTERNATIONAL JOURNAL OF PRECISION ENGINEERING AND MANUFACTURING-GREEN TECHNOLOGY Vol. 3, No. 2, pp. 161-165 APRIL 2016 / 161
DOI: 10.1007/s40684-016-0020-8 ISSN 2288-6206 (Print) / ISSN 2198-0810 (Online)

Study of Electrically-Assisted Indentation for Surface Texturing

Hyun-Seok Oh[1], **Hak-Rae Cho**[1], **Hani Park**[1], **Sung-Tae Hong**[1], and **Doo-Man Chun**[1,#]

1 School of Mechanical Engineering, University of Ulsan, 93, Daehak-ro, Nam-gu, Ulsan, 44610, South Korea
Corresponding Author / Email: dmchun@ulsan.ac.kr, TEL: +82-52-259-2706, FAX: +82-52-259-1680

KEYWORDS: Electrically-Assisted indentation, Vickers hardness, Electric current

Electrically-Assisted manufacturing is a promising hybrid manufacturing process for improved ductility and elongation during plastic deformation of metals and decreased spring-back. Most studies have focused on the deformation of a whole material by applying electric current through the whole material, and many electrically-assisted manufacturing processes including forging, rolling, and sheet metal forming have been introduced. However, plastic deformation processes on a surface, such as indentation, embossing, and scribing, are also important for functional surface texturing and marking, among other uses. In this study, the effect of a continuous electric current on indentation in stainless steel and titanium was investigated using Vickers hardness test. The hardness was decreased by the electric current during indentation with a diamond tip. The amount of decreased hardness depended on the amplitude of the electric current and the positions of two electrodes. The electric current density passing through the surface was calculated by finite element analysis, and the hardness decrease was proportional to the electric current density.

Manuscript received: January 14, 2016 / Revised: March 13, 2016 / Accepted: March 16, 2016

NOMENCLATURE

E = Electric energy (J)
I = Electric current (A)
R = Resistance (Ω)
t = Time duration of electric current (sec)
$\tilde{n}$ = Specific resistance ($\Omega \cdot$m)
l = Distance (m)
A = Area (m^2)
V = Volume (m^3)

1. Introduction

Hybrid manufacturing processes are combinations of manufacturing processes used to produce products in more efficient, effective and productive ways, and there are various different hybrid manufacturing processes.[1-3] Hybrid manufacturing processes can include assisted processes[4-8] or mixed processes[9-12] in order to combine different energy sources or tools.

Electrically-Assisted Manufacturing (EAM) is a hybrid manufacturing process that utilizes electric current, mainly during the plastic deformation of metals and their alloys, to improve productivity, efficiency, and quality at relatively lower temperatures compared to hot working. The mechanical properties of metals and their alloys can change temporarily or permanently under the application of electric currents during plastic deformation. This phenomenon is often referred to as electroplasticity. However, electric currents can cause thermal effects by Joule heating as well as athermal effects by electroplasticity.[13]

EAM processes have been widely utilized in various different manufacturing processes mainly associated with bulk deformation and sheet-metal forming. Electrically-Assisted (EA) forging, EA rolling, and EA drawing as bulk deformation processes could increase deformability and reduce flow stress.[14-16] EA bending, EA deep drawing, and stretch forming as sheet-metal forming could increase deformability and reduce flow stress and springback.[17-19]

Most studies have applied electric current through the whole workpiece, and these were effective for bulk deformation and sheet metal forming. However, this approach is not suitable for local plastic deformation processes such as coining, embossing, and surface texturing. In addition, some researchers have used tools or dies as electrodes to minimize power consumption and unwanted heating. However, tools or dies can easily experience Joule heating and electroplasticity with electric currents.[15,19,20]

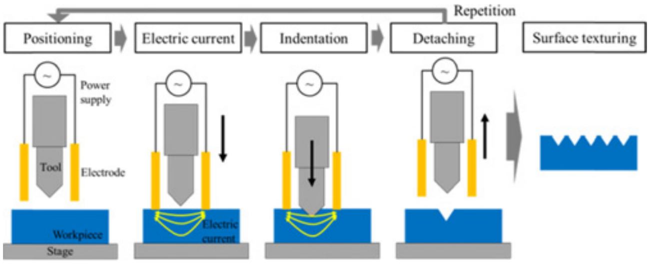

Fig. 1 Schematic procedure of electrically-assisted indentation for surface texturing

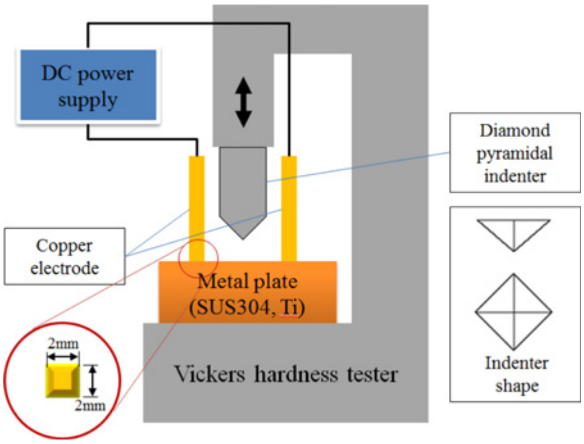

Fig. 2 Schematic image of experimental setup for electrically-assisted indentation using Vickers hardness tester

In this study, electrically-assisted indentation using separated electrodes and local electric current was introduced for surface texturing. The effects of the electric current and the distance from the electrodes to the indentation were studied with a Vickers hardness tester. The electric current density passing through the surface was calculated using finite element analysis, and the measured hardness was compared with the calculated electric current density.

2. Experiment

2.1 Electrically-Assisted Indentation for Surface Texturing

The EA indentation for surface texturing consists of a tool, electrodes, x-y-z stage, electric power supply, sensors and controllers. Fig. 1 shows the configuration and the procedure for EA indentation for surface texturing. First, the tool and electrodes are moved to the position of the indentation, and the electrode contacts are placed on the workpiece. During indentation, the electric current is applied to reduce the indentation load and deepen the indentation. Finally, the electrodes and tool are detached from the workpiece. These procedures are repeated for surface texturing.

2.2 Experimental Setup

To evaluate the effects of continuous electric current on the indentation of hard metal surfaces, the Vickers hardness test was used, because it is reliable and repeatable and is one of the standard hardness tests. In the Vickers hardness test, the diamond indenter as an electric insulation tool and precision load control were suitable for this research. In addition, electrodes with different gaps (6, 8, and 10 mm) were used, and different electric currents (0, 30, 60, and 90 A) were applied from the power supply. Fig. 2 shows the experimental setup for the evaluation of the effects of continuous electric current on surface indentation using the widely utilized hardness test. The experimental setup consists of a Vickers hardness testing machine (HV-114, Mitutoyo, Japan), a DC power supply (EX2500, ODA Technologies, Korea), and a jig with copper electrodes. In this study, stainless steel 304 (SUS304: Nilico Corporation, Japan) and titanium (99.5% purity, Nilico Corporation, Japan) were selected because they have hard surfaces and wide applications. The thicknesses of both types of metal plate were 5 mm: their surfaces were polished with diamond slurry and the surface roughness (Ra) values of the SUS304 and titanium were about 0.1 μm and 0.4 μm, respectively. Vickers hardness tests were carried out five times for each combination of electrode gap and electric current. The experimental conditions are summarized in Table 1. The indentation marks were measured by confocal microscopy (VK-X200, Keyence, Japan) for precise measurements of hardness and depth. Fig. 3 shows the indentation marks after hardness tests were

Table 1 Experimental conditions for Vickers hardness testing with electric currents

Condition	Value
Indentation load (N)	20
Indentation time (sec)	20
Time for electric current (sec)	20
DC electric current (A)	0, 30, 60, 90
Distance between electrodes (mm)	6, 8, 10

(a) SUS 304

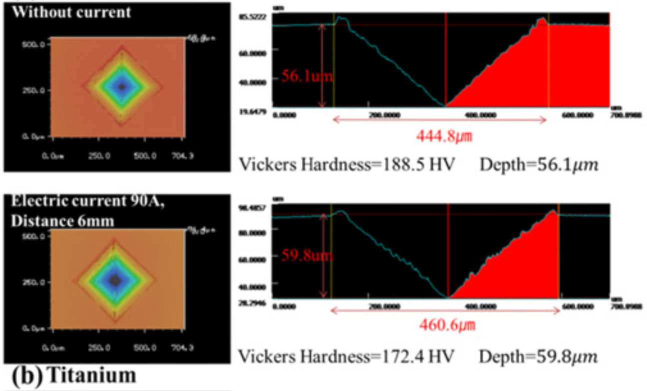

(b) Titanium

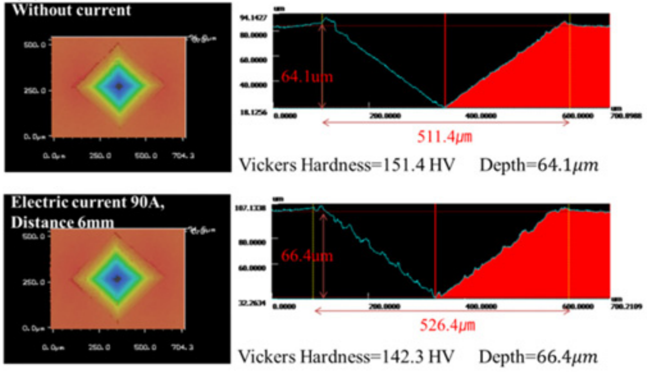

Fig. 3 Confocal microscope images of impression diagonals produced by pyramidal indenter: (a) Stainless steel plates, (b) Titanium plates without/with a 90-A electric current and a distance of 6 mm between two electrodes

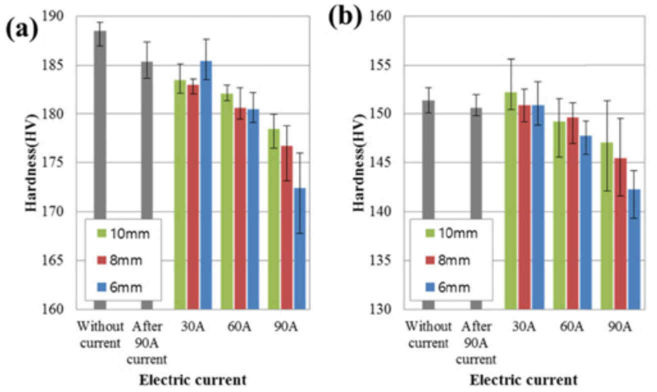

Fig. 4 Changes in Vickers hardness with electric current: (a) SUS304, (b) Titanium

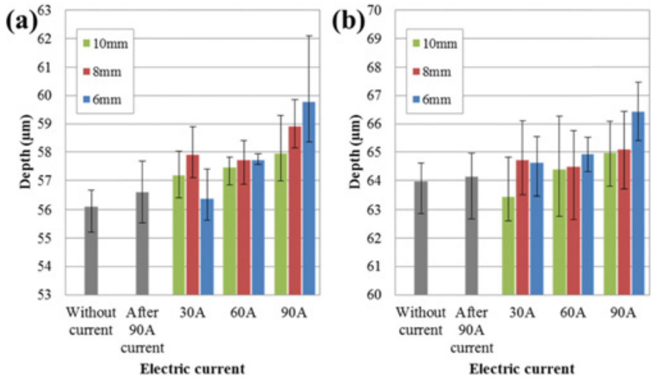

Fig. 5 Changes in indentation depths with electric current: (a) SUS304, (b) Titanium

conducted on plates without electric current and with an electric current of 90 A and an electrode gap of 6 mm. The diamond indenter tip was projected on the metal surface, and the electric current helped to create wider and deeper indentation marks on both metals.

2.3 Experimental Result

Measured hardness results are summarized in Fig. 4. As a reference value, the hardness without electric current was measured. Then, the hardness with electric currents (30, 60, and 90 A) was measured by changing the distance (6, 8, and 10 mm) between the two electrodes. Under 90 A of electric current, hardness reductions were clearly observed, and the effect of the distance between the two electrodes became dominant. Furthermore, the hardness reduction was increased as the electrode gap was decreased on both the SUS 304 and titanium plates. In addition, the hardness was measured after a 90-A electric current was applied with 6 mm of distance between the two electrodes without indentation to confirm any permanent effects of the electric current alone. The difference in hardness between the reference and this case was negligible in the titanium plate, but the SUS304 plate showed a small difference within the error range. The results for indentation depth showed similar trends. As the electric current increased and the distance between the electrodes decreased, the depth increased, as shown in Fig. 5. As a result, a 9.1% hardness reduction and 6.7% depth increase were achieved on SUS304 with a 90-A electric current and 6-mm electrode gap, and a 7.2% hardness reduction and 5.1% depth increase on titanium were achieved with under the same conditions.

Table 2 Parameters of finite element analysis for electric current calculation

Information	Value
Software	ANSYS 14 workbench
Resistance (Ohm-m)	7.2e-08 (SUS304) 1.7E-06 (Titanium)
Mesh size (mm)	0.5
DC electric current (A)	30, 60, 90
Distance between electrodes (mm)	6, 8, 10

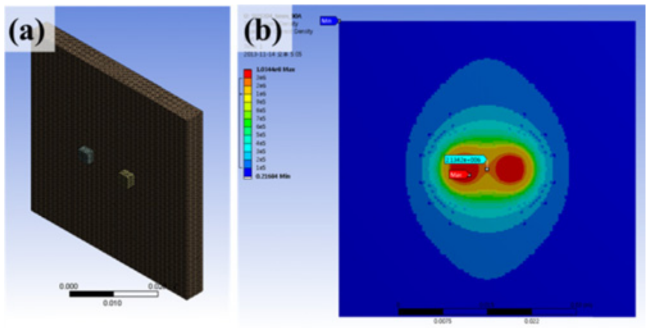

Fig. 6 Finite element method for calculation of electric current density: (a) Mesh model, (b) Current density results of SUS304 with 90-A current

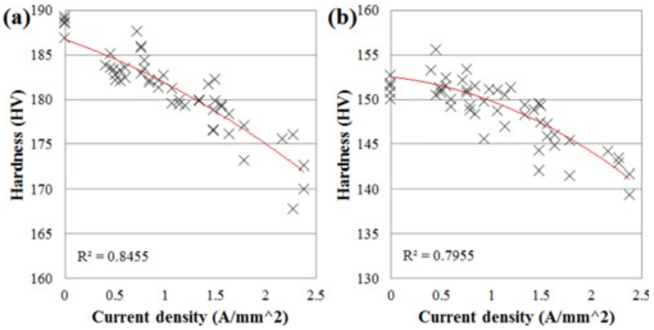

Fig. 7 Vickers hardness with current density: (a) SUS304, (b) Titanium

3. Discussion

The current density and electric energy density are important parameters in the effects of electric current on mechanical properties.[21] When the electric current moves through the constant cross-sectional area of a conductor such as the specimens for a tensile test or bending test, the current density can be calculated easily. However, the electric current density cannot be easily calculated for this research because the electric current density depends on the positions and geometries of the electrodes and substrate. To understand the effects of the electric current and the distance between the two electrodes, the commercial finite element analysis software, ANSYS 14 Workbench for electric models, was used. Table 2 summarizes the input parameters of the finite element analysis model for electric current calculations. Three different models of the different distances between electrodes with three different electric currents were simulated. The simulation results were steady state and the resistance was assumed to be constant. Fig. 6 shows the simulation model. The electrodes were simplified as short square shapes (2 × 2 mm^2), and the contacts between the electrodes and substrate were simplified as perfect contacts. The electric current

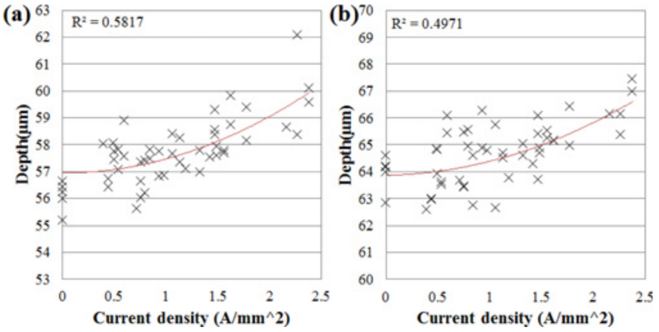

Fig. 8 Indentation depth with current density: (a) SUS304, (b) Titanium

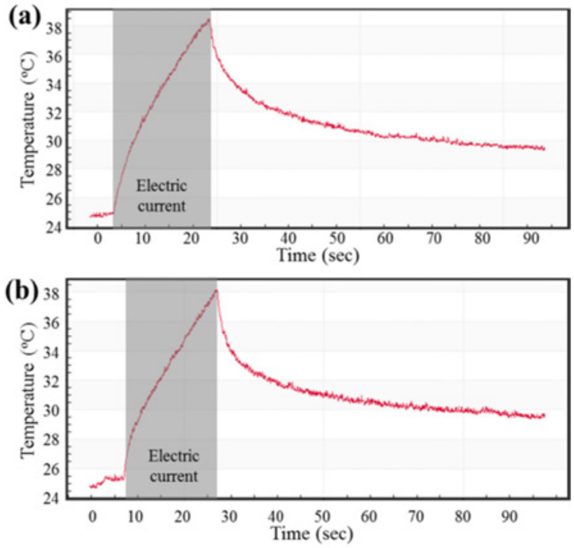

Fig. 9 Temperature changes according to time with an electric current of 90 A and electrode distance of 6 mm applied for 20 seconds: (a) SUS304, (b) Titanium

density depends on the position, but the results were derived from the center point between the two electrodes.

The measured Vickers hardness results with the calculated current densities were plotted as shown in Fig. 7. The hardness results were reversely proportional to the current densities. The energy provided to a specific volume is important and may be proportional to the reduction of hardness. The electric energy can be calculated as given in Eq. (1), and resistance can be calculated as in Eq. (2) with constant specific resistance. Finally, the electric energy density due to the electric current can be expressed as in Eq. (3).

$$E = I^2 \cdot R \cdot t \tag{1}$$

$$R = \rho \frac{l}{A} \tag{2}$$

$$\frac{E}{V} = \left(\frac{I}{A}\right)^2 \cdot \rho \cdot t \tag{3}$$

Here, ρ and t were assumed to be constants, because the applied current was constant and the time duration of the electric current was fixed at 20 seconds. Based on Eq. (3), the trend line was set as a second-order polynomial with electric current density. Even though there was a relatively large deviation, because the indentation was not a point and the material properties depended on the position and depth, this polynomial could represent the clear relationship between measured hardness and electric current density. Fig. 7 shows the relationship between the measured hardness and the calculated electric current density on the SUS304 and titanium substrates. As the current density increased, the hardness decreased.

The indentation depth was also compared with current density, as shown in Fig. 8. The trend was almost the same as that of hardness, but it was less clear than that of hardness. Under the same indentation load (20 N), the electric current improved the indentation depth. For surface texturing, a deep texture can be obtained with electric current.

Electric current can generate heat as Joule heating and then the generated heat can increase the temperature of the substrate. Under high temperatures, mechanical properties such as Young's modulus and yield strength decrease due to thermal softening, so the reduction in hardness and increase in indentation depth seem to be obvious results, as observed in hot working processes. However, electric current can be used for two different phenomena, a thermal effect (Joule heating) and an athermal effect (electroplasticity) in EAM, and electroplasticity can be observed at relatively low temperatures. To assess the effects of temperature, the temperature changes on the surface during the application of electric current under the most severe conditions (90 A of electric current and a 6-mm electrode gap) were measured with an infrared thermal imaging camera (FLIR-T621, FLIR Systems, Sweden), as shown in Fig. 9. The gray region indicates the applied electric current. The maximum temperatures around the center between the two electrodes were 38.5 and 38°C on SUS304 and titanium, respectively. The measured temperatures were too low to suggest that thermal softening alone affected the hardness reduction. In addition, the maximum temperatures were not sustained for long, and the average temperatures were much lower than the maximum temperatures.

4. Conclusions

We proposed the concept of electrically-assisted indentation for surface texturing and studied the effects of electric current on the diamond tool indentation with a Vickers hardness tester. As expected, the hardness decreased as the electric current increased and the distance between the electrodes decreased. The hardness change was proportional to the electric current density, which was calculated via finite element analysis. The relationship was explained by the specific electric energy. As the electric current density increased, the hardness decreased and the indentation depth increased. When the electric current was held constant, the effect was improved by reducing the distance between the electrodes. In addition, the process temperature was low, and unnecessary heating was prevented by using a local electric current.

In this study, a continuous current was used to show the feasibility of hardness reduction and low heating with easy calculation of electric current density. In the future, a pulse type of electric current will be studied, because the pulse type is known to be an effective method for electroplasticity that can minimize power consumption and heating effects.

ACKNOWLEDGEMENT

This work was supported by the National Research Foundation of Korea (NRF) grant funded by the Korean government (NRF-2015R1C1A1A02036321)

REFERENCES

1. Lauwers, B., Klocke, F., Klink, A., Tekkaya, E., Neugebauer, R., et al., "Hybrid Processes in Manufacturing," CIRP Annals-Manufacturing Technology, Vol. 63, No. 2, pp. 561-583, 2014.
2. Zhu, Z., Dhokia, V. G., Nassehi, A., and Newman, S. T., "A Review of Hybrid Manufacturing Processes-State of the Art and Future Perspectives," International Journal of Computer Integrated Manufacturing, Vol. 26, No. 7, pp. 596-615, 2013.
3. Chu, W.-S., Kim, C.-S., Lee, H.-T., Choi, J.-O., Park, J.-I., et al., "Hybrid Manufacturing in Micro/Nano Scale: A Review," Int. J. Precis. Eng. Manuf.-Green Tech., Vol. 1, No. 1, pp. 75-92, 2014.
4. Kim, J.-H., Choi, J.-Y., and Lee, C.-M., "A Study on the Effect of Laser Preheating on Laser Assisted Turn-Mill for Machining Square and Spline Members," Int. J. Precis. Eng. Manuf., Vol. 15, No. 2, pp. 275-282, 2014.
5. Lee, S.-J., Kim, J.-D., and Suh, J., "Microstructural Variations and Machining Characteristics of Silicon Nitride Ceramics from Increasing the Temperature in Laser Assisted Machining," Int. J. Precis. Eng. Manuf., Vol. 15, No. 7, pp. 1269-1274, 2014.
6. Sim, M.-S. and Lee, C.-M., "A Study on the Laser Preheating Effect of Inconel 718 Specimen with Rotated Angle with Respect to 2-Axis," Int. J. Precis. Eng. Manuf., Vol. 15, No. 1, pp. 189-192, 2014.
7. Ahn, S. H., Choi, J. O., Kim, C. S., Lee, G. Y., Lee, H. T., et al., "Laser-Assisted Nano Particle Deposition System and Its Application for Dye Sensitized Solar Cell Fabrication," CIRP Annals-Manufacturing Technology, Vol. 61, No. 1, pp. 575-578, 2012.
8. Lin, Y.-C., Chuang, F.-P., Wang, A. C., and Chow, H.-M., "Machining Characteristics of Hybrid EDM with Ultrasonic Vibration and Assisted Magnetic Force," Int. J. Precis. Eng. Manuf., Vol. 15, No. 5, pp. 1143-1149, 2014.
9. Cho, Y. T. and Na, S. J., "Numerical Analysis of Plasma in CO_2 Laser and ARC Hybrid Welding," Int. J. Precis. Eng. Manuf., Vol. 16, No. 4, pp. 787-795, 2015.
10. Cao, X. D., Kim, B. H., and Chu, C. N., "Hybrid Micromachining of Glass Using ECDM and Micro Grinding," Int. J. Precis. Eng. Manuf., Vol. 14, No. 1, pp. 5-10, 2013.
11. Ahn, S. H., Chun, D. M., and Kim, C. S., "Nanoscale Hybrid Manufacturing Process by Nano Particle Deposition System (NPDS) and Focused Ion Beam (FIB)," CIRP Annals-Manufacturing Technology, Vol. 60, No. 1, pp. 583-586, 2011.
12. Park, C., Shin, B.-S., Kang, M.-S., Ma, Y.-W., Oh, J.-Y., et al., "Experimental Study on Micro-Porous Patterning Using UV Pulse Laser Hybrid Process with Chemical Foaming Agent," Int. J. Precis. Eng. Manuf., Vol. 16, No. 7, pp. 1385-1390, 2015.
13. Nguyen-Tran, H.-D., Oh, H. S., Hong, S.-T., Han, H. N., Cao, J., et al., "A Review of Electrically-Assisted Manufacturing," Int. J. Precis. Eng. Manuf.-Green Tech., Vol. 2, No. 4, pp. 365-376, 2015.
14. Jones, J. J., Mears, L., and Roth, J. T., "Electrically-Assisted Forming of Magnesium AZ31: Effect of Current Magnitude and Deformation Rate on Forgeability," Journal of Manufacturing Science and Engineering, Vol. 134, No. 3, Paper No. 034504, 2012.
15. Zhu, R., Tang, G., Shi, S., and Fu, M., "Effect of Electroplastic Rolling on the Ductility and Superelasticity of TiNi Shape Memory Alloy," Materials & Design, Vol. 44, pp. 606-611, 2013.
16. Tang, G., Zhang, J., Zheng, M., Zhang, J., Fang, W., et al., "Experimental Study of Electroplastic Effect on Stainless Steel Wire 304L," Materials Science and Engineering: A, Vol. 281, No. 1-2, pp. 263-267, 2000.
17. Green, C. R., McNeal, T. A., and Roth, J. T., "Springback Elimination for Al-6111 Alloys Using Electrically-Assisted Manufacturing (EAM)," North American Manufacturing Research Institution of SME, Vol. 37, pp. 403-410, 2009.
18. Wang, S., "Effect of Electric Pulses on Drawability and Corrosion Property of AZ31 Magnesium Alloy," M.Sc. Thesis, Materials Science and Engineering, Tsinghua University, 2009.
19. Jones, J. J. and Mears, L., "A Process Comparison of Simple Stretch Forming Using both Conventional and Electrically-Assisted Forming Techniques," Proc. of ASME International Manufacturing Science and Engineering Conference, Paper No. MSEC2010-34144, pp. 623-631, 2010.
20. Asghar, J. and Reddy, N., "Importance of Tool Configuration in Incremental Sheet Metal Forming of Difficult to Form Materials Using Electro-Plasticity," Proc. of the World Congress on Engineering, Vol. 3, 2013.
21. Roh, J. H., Seo, J. J., Hong, S.-T., Kim, M. J., Han, H. N., et al., "The Mechanical Behavior of 5052-H32 Aluminum Alloys under a Pulsed Electric Current," International Journal of Plasticity, Vol. 58, pp. 84-99, 2014.